

1
2
3
4 **Impact of Desalination on the General Circulation of the Arabian Gulf:**
5
6 **Present and Future Scenarios**
7
8

9
10 1 **Maryam R. Al Shehhi^{1*}, Hajoon Song^{2,3*}, Jeffery Scott⁴, Fahim Abdul Gafoor¹ and**
11 2 **John Marshall⁴**
12

13
14 3 ¹Department of Civil Infrastructure and Environmental Engineering, Khalifa University of
15 4 Science and Technology, Abu Dhabi, United Arab Emirates
16

17 5 ²Department of Atmospheric Sciences, Yonsei University, Seoul, Korea
18

19 6 ³Division of Environmental Science & Engineering, Pohang University of Science and
20 7 Technology, Pohang, Republic of Korea
21

22 8 ⁴Earth, Atmospheric and Planetary Science Department, Massachusetts Institute of
23 9 Technology, 77 Massachusetts Ave., Cambridge, MA 02139, USA
24
25

26
27
28 *** Correspondence:**
29

30 11 Corresponding Authors: Maryam R. Al Shehhi: maryamr.alshehhi@ku.ac.ae; Hajoon Song:
31 12 hajsong@yonsei.ac.kr
32
33

34
35 13 **Keywords: Brine Discharge; Desalination; Ocean Impacts; Sea of Oman; Indian Ocean;**
36 14 **Saline Outflow; MITgcm**
37
38

39 15
40
41
42 16
43
44 17
45
46 18
47
48 19
49
50
51 20
52
53 21
54
55 22
56
57
58 23
59
60 24
61
62
63
64
65

1
2
3 25
4
5
6 26
7
8 27
9 28
10
11 29
12
13 30
14
15 31
16
17 32
18
19 33
20 34
21
22 35
23
24 36
25
26 37
27
28
29 38
30
31
32
33
34
35
36
37
38
39
40
41
42
43
44
45
46
47
48
49
50
51
52
53
54
55
56
57
58
59
60
61
62
63
64
65

Abstract

By 2050, freshwater production from desalination plants is expected to increase sixfold. Currently, over 850 desalination plants operate in the Arabian Gulf, with significant local impacts from brine discharge, especially along the southwestern coast. This study uses a km-scale resolution ocean model of the Gulf and Sea of Oman, to investigate the impact of increased salinity on the circulation and water-mass transformation within the Gulf under different desalination forcing scenarios, ranging from no desalination plants to an extreme 50-times present levels of desalination. As the forcing is enhanced, increases in salinity and temperature are found, especially near the bottom of the Gulf as salty, warm dense waters sink to depth. However, efficient water exchange through the Strait means that even in extreme desalination scenarios, large-scale changes in temperature and salinity are muted. Local impacts near plants are more pronounced, with increased water-mass transformation, deepening, and strengthening of overturning circulation.

1
2
3 39 **Key findings:**
4

5
6 40 **1.** Surface salinity increases in the environs of desalination plants in the Arabian Gulf, and its
7
8 41 waters become generally saltier, warmer and denser, particularly near the bottom and on the
9
10 42 southern shoreline.

11
12 43 **2.** The exchange between the Gulf and the Sea of Oman through the Strait of Hormuz,
13
14 44 strengthens and deepens with enhanced outflow of warm salty water and stronger inflow at the
15
16 45 surface, damping the large-scale effects of desalination.

17
18 46 **3.** Increases in desalination rates of up to 50-times current levels are considered, at which point
19
20 47 subsurface temperatures and salinity along the southern shoreline change by roughly 0.6 °C
21
22 48 and 2 g/kg, respectively, with a 20% increase in exchange rates through the Strait.
23

24
25 49
26
27 50 **1. Introduction**
28

29 51 Due to limited freshwater resources, many countries depend on desalination plants to provide
30
31 52 fresh water for domestic and industrial purposes. Although such plants meet an urgent need,
32
33 53 insufficient dilution of salty discharge into the marine environment can negatively affect
34
35 54 marine habitats such as corals and seaweed meadows (Danoun, 2007). Around half of the
36
37 55 world's desalination plants are located in the arid regions of the Middle East, surrounding the
38
39 56 Arabian Gulf (Roberts et al., 2010; Hosseini et al., 2021), which has an estimated desalination
40
41 57 capacity of 11 million cubic meter of fresh water per day. This production capacity comes
42
43 58 from more than 200 active desalination plants along the shallow western and southern shore
44
45 59 of the Gulf (Figure 1), and 51 additional ones are expected to be commissioned in the near
46
47 60 future (Sharifinia et al., 2019; Hosseini et al., 2021; Purnama, 2021). With the increase in
48
49 61 population, there is a plan to double desalination along Arabian coast by 2050. As shown in
50
51 62 Figure 1, the cumulative projected desal capacity in 2050 is 80 million m³ day⁻¹ which is more
52
53 63 than double of that in 2020 and eight times that in 2010 (Le Quesne et al., 2021).

54 64 Although seawater desalination is an effective solution to the scarcity of fresh water, it puts
55
56 65 pressure on the marine ecosystem especially in coastal areas. The salinity of brine discharge
57
58 66 is typically up to twice that of the ambient seawater (i.e. 50-70 psu compared to ~35 psu) (Abd
59
60 67 El Wahab and Hamoda, 2012) (Panagopoulos et al., 2019). Since the density of discharge is
61
62 68 largely determined by its salinity, it often sinks to the bottom with little mixing (Einav et al.,
63

2003). Moreover, since discharge takes place in a coastal zone in the presence of complex ocean currents (Ruso et al., 2007; Sola et al., 2020) it tends to sink down and spread along the seabed, the details depending on outfall design and the mixing and flushing characteristic of the local area. Note also that brine outflows from desalination plants can exceed seawater ambient temperature (Missimer and Maliva, 2018), depending on the desalination technology employed; however, we do not attempt to capture this impact, rather our impetus is modeling and understanding the non-local impacts of increased salinity at the plants' locations.

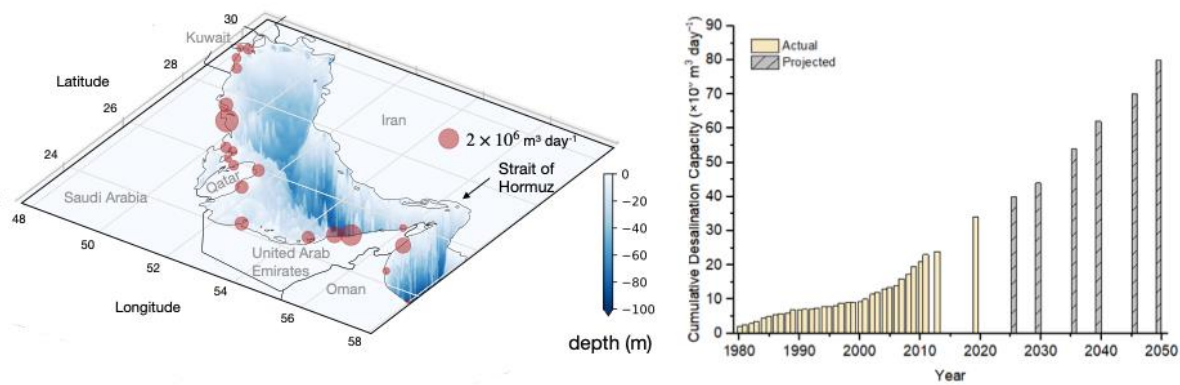


Figure 1. (left) The location of major desalination plants along the coast of the Arabian Gulf are presented by the red circles. The size of the circles corresponds to the capacity of freshwater produced from each desalination plant. Blue represents the bathymetry of the Gulf, ranging from shallow (shaded light) waters to 100 m deep (shaded dark). (right) Cumulative desalination capacity around the Arabian Gulf ($1 \times 10^6 \text{ m}^3 \text{ day}^{-1}$) between 1980 to 2020 and the projection between 2020 to 2050. The desalination plant dataset was obtained from the DesalData database (<http://www.desaldata.com>).

Most studies of environmental impacts have been carried out in support of acquiring permits from the relevant authorities with a focus on local effects. For example previous studies report salinity increases up to 2 psu within 20 m of the outlet, decaying to 0.8 psu at a distance of 100 m or so (Roberts et al., 2010; Clark et al., 2018), with concomitant temperature increase up to 0.7 K (Kress et al., 2020). However, individual outfalls have individual footprints, which depend on flow rates, effluent characteristics and outfall design. There have been fewer studies of the wider implications of desalination on the large-scale circulation of the Gulf. Ibrahim & Eltahir (2019) used a high-resolution coupled Gulf Atmosphere Regional Model (GARM) and found that flushing by the residual circulation inhibited salt buildup on the scale of the basin. Campos et al. (2020) found that velocities in the deep channel of the Strait of Hormuz

1
2
3 96 increased by 0.20 m s^{-1} when the impact of brine discharge is considered. Paparella et al.
4
5 97 (2022) applied atmospheric forcing based on the IPCC SSP5-8.5 scenario, which projected
6
7 98 reduced evaporation rates, increased air temperature, and higher precipitation in the Arabian
8
9 99 Gulf, considering the presence of desalination plants. They found that it is unlikely for the
10
11 100 average salinity of the Gulf to increase by more than 1 psu and, under less extreme conditions,
12
13 101 it will likely remain well below 0.5 psu, with negligible environmental impacts.

14
15 102 There remains a need to explore the large-scale implications of salinization on the
16
17 103 oceanography of the Gulf, the water mass transformation going on within it, associated vertical
18
19 104 overturning circulation and exchange with the Sea of Oman through the Strait of Hormuz. To
20
21 105 that end we take a high-resolution model of the circulation of the region with a good and
22
23 106 documented climatology – the model is described in Al Shehhi et al. (2021) – and perturb it
24
25 107 with salinity sources associated with the desalination plants shown in Figure 1. We then
26
27 108 imagine that the desalination stress on the ocean is increased 10-fold, 20-fold etc. and, in an
28
29 109 extreme case, up to 50-fold over present-day values. We document how circulation,
30
31 110 stratification, hydrography and exchange properties change relative to the unperturbed state,
32
33 111 and the patterns of those changes. By exploring extreme cases we can study the inherent
34
35 112 robustness of the system and the key ways in which the Gulf could change. We conclude that
36
37 113 the large-scale circulation and patterns of flow are rather robust even in extreme desalination
38
39 114 scenarios and the salinity response, although locally large, is ameliorated on the basin scale
40
41 115 through the efficient exchange between the Gulf and the Sea of Oman which acts to mute
42
43 116 change.

44 45 46 118 **2 Modeling framework and implementation**

47 48 49 119 **2.1 Model setup and climatology**

50
51
52 120 The high resolution three-dimensional hydrodynamic model of the Arabian Gulf described in
53
54 121 Al Shehhi et al. (2021) is used in this study. It is based on the Massachusetts Institute of
55
56 122 Technology’s general circulation model (MITgcm) (Marshall et al., 1997). The model domain
57
58 123 extends from the Arabian Gulf to the Sea of Oman. The model bathymetry is obtained from
59
60 124 the 1-min Smith and Sandwell Global Topography dataset (Smith and Sandwell, 1997) as
61
62 125 indicated by the blue shading in Figure 1. The model grid has a quasi-uniform horizontal

1
2
3 126 resolution of 2.5 km with 83 layers in the vertical, much thinner (order 1 m) at the surface than
4
5 127 in the abyss. There are 25 layers in the Gulf. Initial and boundary values of zonal and
6
7 128 meridional velocity components, temperature, salinity, and sea surface height were obtained
8
9 129 from a global ocean MITgcm simulation LLC4320 with the same resolution in horizontal and
10
11 130 vertical (Rocha et al., 2016). Boundary conditions were imposed at the southern and eastern
12
13 131 boundaries in the Sea of Oman including surface elevation and currents associated with eight
14
15 132 tidal constituents (K2, S2, M2, N2, K1, P1, O1, Q1) derived from a global tidal model (Tidal
16
17 133 Prediction eXternal Software: TPXO) (Egbert et al., 1994). The model was forced from above
18
19 134 by 6 hourly reanalysis data sourced from the European Centre for Medium-Range Weather
20
21 135 Forecasts (ECMWF) at a spatial resolution of 0.14°. The reanalysis data includes downward
22
23 136 short and longwave radiation, precipitation, wind components at a height of 10 m together with
24
25 137 the 2 m temperature and dew point. Runoffs from four rivers – the Shatt Al-Arab, Hendijan,
26
27 138 Hilleh, and Mand – are also included. The simulation is for the repeating year 2012, with a
28
29 139 spin up of 6 years at which time the initial state of the model is ‘forgotten’.

30
31 140 The climatology of the model is documented in detail in Al Shehhi et al. (2021), where it is
32
33 141 compared with a range of observations, both in-situ and remotely sensed. We show some key
34
35 142 fields of model climatology in Figure 2. The simulated sea surface temperature varies from 22
36
37 143 °C in the north to 28 °C in the southeastern region of the Gulf toward the Sea of Oman (Figure
38
39 144 2(a)). The surface annual-mean salinity (S) of our solution shown in Figure 2(b) reveals that,
40
41 145 as expected, the interior Gulf is generally saltier than the waters of the Sea of Oman and is the
42
43 146 saltiest in the inner Gulf and along the south coast where salinity can exceed 45 psu (g/kg).
44
45 147 This is a reflection of the fact that the Gulf is an evaporative basin and the inflow through the
46
47 148 Strait of Hormuz comprises relatively fresh water.

48
49 149 Figure 2(c,d) show the residual overturning circulation in the zonal and meridional planes,
50
51 150 respectively. In the zonal vertical plane, we observe water being drawn into the Gulf at the
52
53 151 surface and out at depth (negative indicates anticlockwise circulation in the zonal vertical
54
55 152 plane). In the meridional plane, there is also a tendency for water to upwell in the central Gulf
56
57 153 and then move southward toward the south coast where it sinks to depth before outflowing
58
59 154 through the Strait of Hormuz. The underlying dynamics and associated water mass
60
61 155 transformation is described in Al Shehhi et al. (2021). The ability of the model to represent

1
2
3156
4
5
6
7
8
9
10
11
12
13
14
15
16
17
18
19
20
21
22
23
24
25
26
27
28
29
30
31
32
33
34
35
36
37
38
39
40
41
42
43
44
45
46
47157
48
49
50158
51159
52
53160
54161
55162
56
57
58163
59164
60
61
62
63
64
65

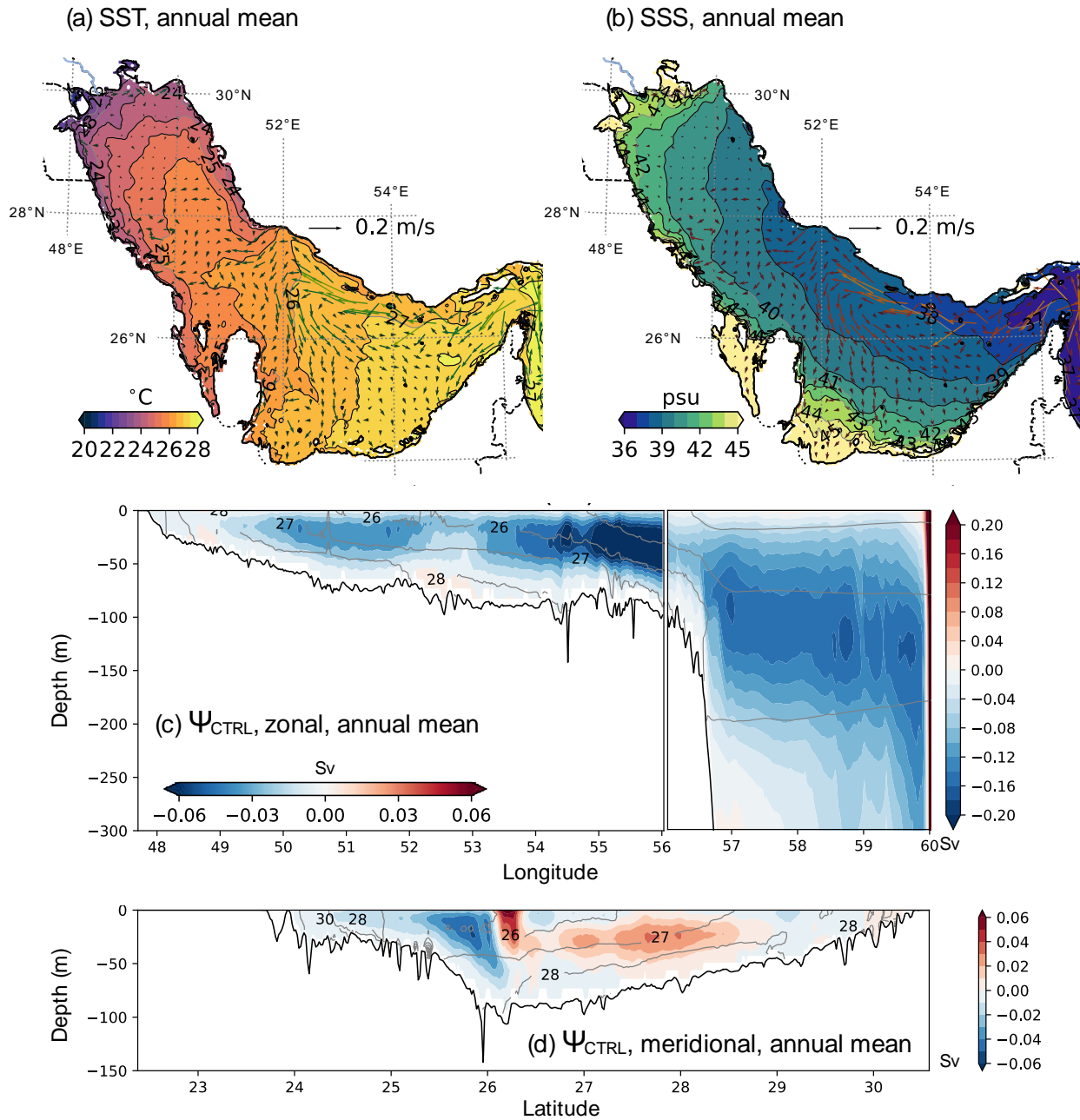


Figure 2. The mean (a) SST and (b) SSS with the surface current from the climatology simulation. (c) and (d) are the mean zonal and meridional residual overturning streamfunction (Ψ), respectively. It is noted that the color scales of the zonal residual streamfunction in (c) are different in the Arabian Gulf and the Sea of Oman. There is anticlockwise (clockwise) circulation around the blue (red) streamfunction.

1
2
3 165 tides and their role in the general circulation are also described in Salim et al (2024) and
4
5 166 Subeesh MP (2024). This base model is now perturbed by various desalination scenarios and
6
7 167 changes monitored and documented. The initial conditions are the same in each scenario.
8

9 168 Desalination Scenarios

10
11
12 169 We have implemented six desalination scenarios: no desalination activities (CTRL), 1-fold
13
14 170 (x1, with salinity forcing implemented to mimic plants shown in Figure 1), 10-fold (x10), 20-
15
16 171 fold (x20), 35-fold (x35) and a 50-fold (x50) increase in forcing. As shown in Figure 1, the
17
18 172 desalination plants are considered. To estimate local salinity impacts from desalination plants,
19
20 173 we used reported plant brine discharge rates (Alosairi and Pokavanich 2017) and assumed that
21
22 174 the freshwater removal rate was equal to the discharge rate (in essence, a freshwater recovery
23
24 175 rate of 50%). Note this is a somewhat higher removal rate than typical achieved (which is
25
26 176 typically 15-40%). Moreover, some of the freshwater produced is returned to the Gulf in the
27
28 177 form of wastewater. We should therefore interpret our forcing as an “upper bound” of the true
29
30 178 desalination impact, in keeping with the idealized, broad nature of our study. Desalination
31
32 179 forcings were implemented by changing the applied E-P-R (evaporation, precipitation, runoff)
33
34 180 at desalination plant locations corresponding to the red circles shown in Figure 1. One way of
35
36 181 thinking of this is that the desal plants are being represented as “negative freshwater rivers”.
37
38 182 As noted previously, no attempt is made to represent any direct temperature effect of the
39
40 183 desalination plants.
41
42
43
44
45
46
47
48
49
50
51
52
53
54
55
56
57
58
59
60
61
62
63
64
65

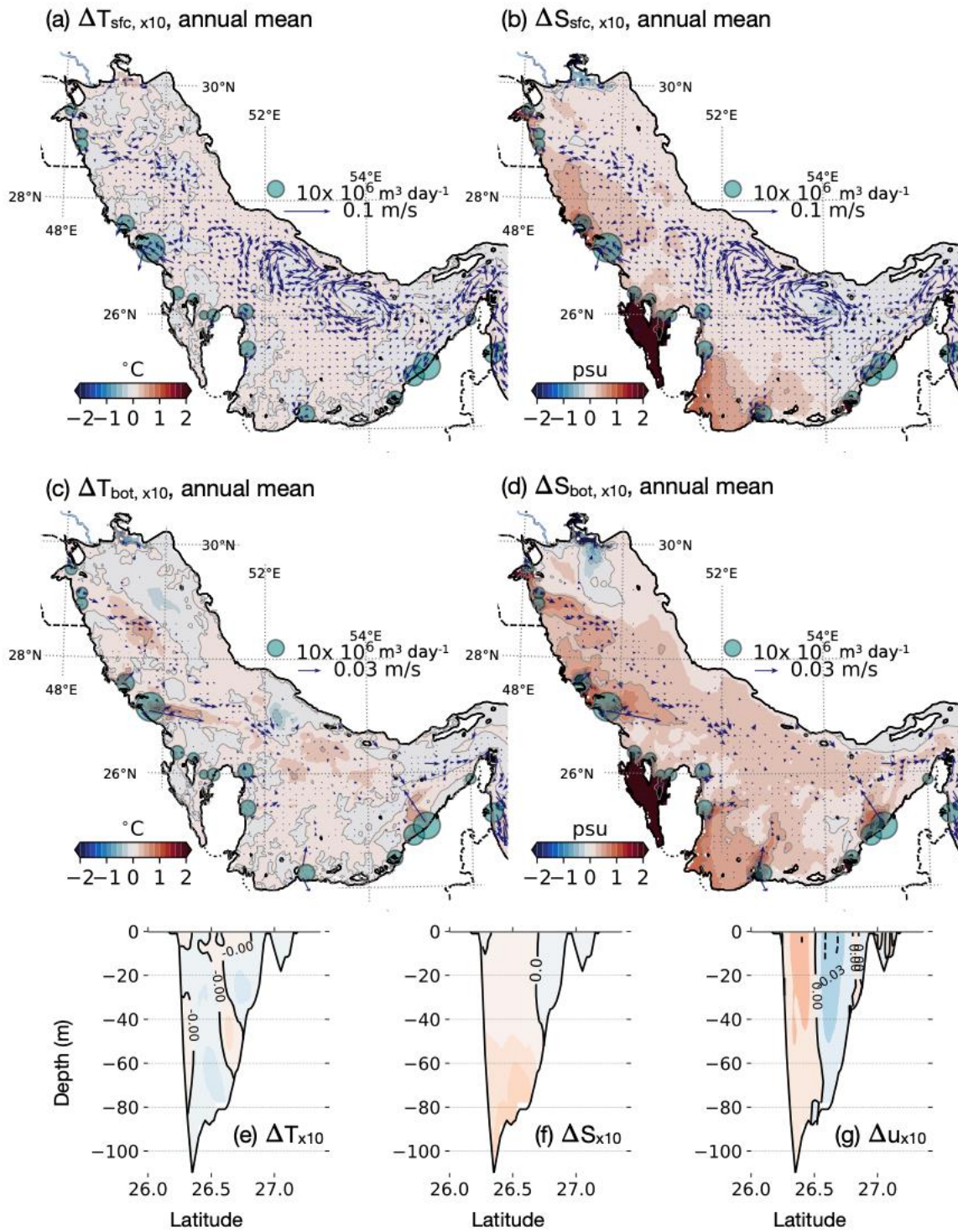


Figure 3. Changes of (a) SST, (b) SSS, (c) bottom temperature and (d) bottom salinity between x10 and CTRL are color shaded, while arrows represent changes in flow at those

1
2
3187
4188
5
6
7
8
9
10
11
12
13
14
15
16
17
18
19
20
21
22
23
24
25
26
27
28
29
30
31
32
33
34
35
36
37
38
39
40
41
42
43
44
45
46
47
48
49
50
51
52
53
54
55
56
57
58
59
60
61190
62
63
64
65

levels. (e-f) show anomalies of T, and zonal flow, respectively, at the Strait of Hormuz. The circles in (a-d) represent the capacity of the desalination plants in x10 simulation.

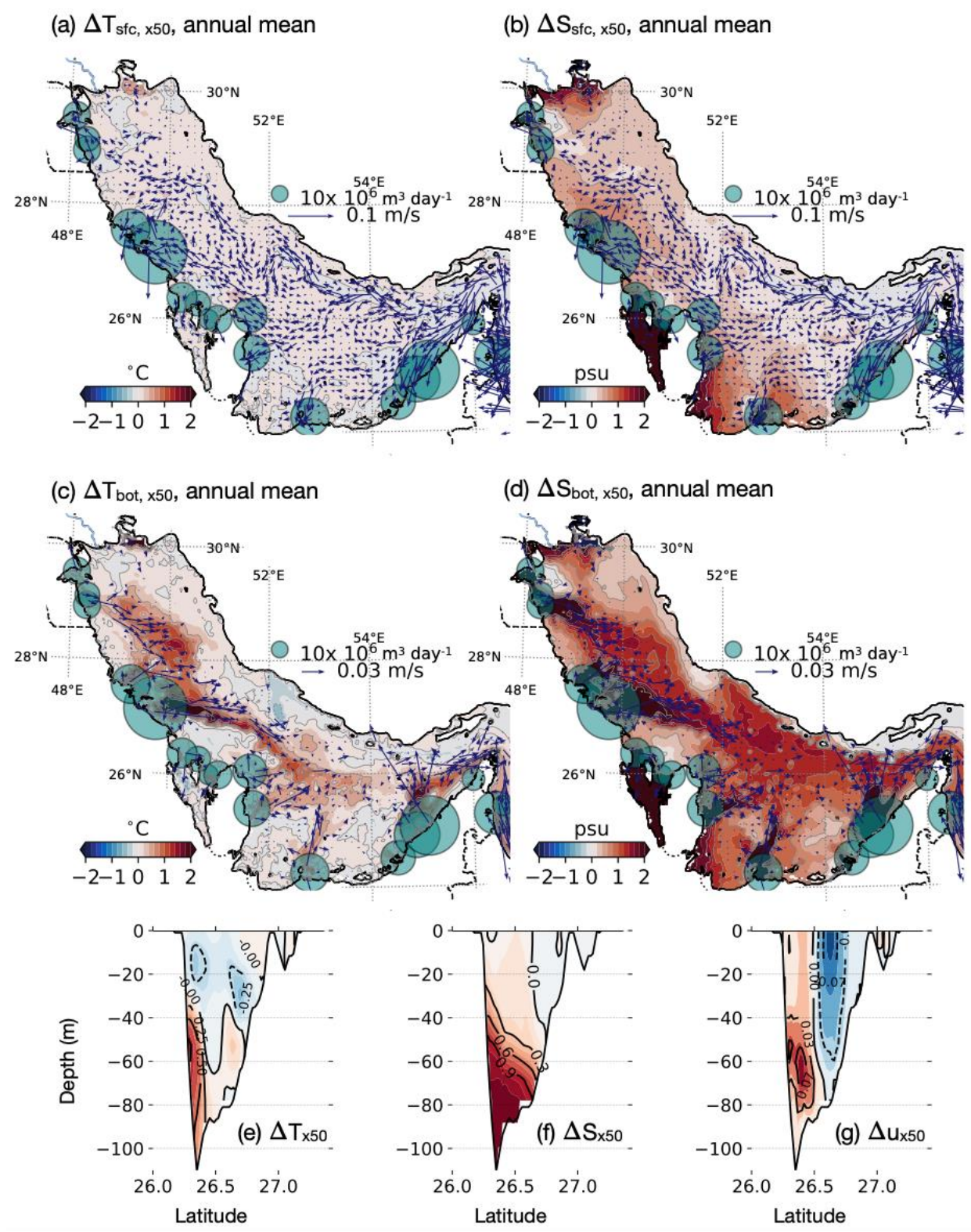


Figure 4. Same as Figure 3, except the changes are between x50 and CTRL.

1
2
3191 **3. Impact of salinity forcing on the circulation, hydrography and overturning**
4
5192 **circulation in the Gulf**
6

7
8193 We first discuss changes in the large-scale pattern of currents and exchange between the Gulf
9
10194 and the Sea of Oman through the Strait of Hormuz. We go on to discuss changes in the
11195 temperature and salinity properties of the Gulf and its zonal and meridional overturning
12
13196 circulations.

14
15
16197 **3.1 Surface ocean currents and exchange**
17

18
19198 The desalination plants result in anomalous surface and bottom currents in the Gulf, and the
20
21199 size of anomalies tends to be larger with the capacity of the desalination plants (Figure 3(a-d)
22200 and 4(a-d)). In x10, we observe an anomalous gyres near the northern, deeper parts of the Gulf
23
24201 (26°N-28°N and 52°E-54°E), but there are also anomalous surface flows towards the sites of
25
26202 desalination plants (Figure 3(a,b)). They are more evident in the x50 case, showing stronger
27
28203 inflow through the Strait of Hormuz into Gulf along the northern coast before being supplied
29
30204 to the desalination plants (Figure 4(a,b)). The size of these anomalous flows can be significant,
31
32205 approximately 50% of the surface current in CTRL.

33
34206 The anomalous bottom currents in the Gulf generally flow out from the desalination plants
35
36207 towards the Strait of Hormuz (Figure 3(c,d) and 4(c,d)). These currents are strongest near the
37
38208 desalination plants and flow down the slope of the bathymetry. Again, the anomalous bottom
39
40209 currents are more pronounced in x50, which carry the warm and salty water mass towards the
41
42210 Sea of Oman. Hence, the desalination plants have the potential to ‘draw’ the surface fluid in
43
44211 towards them where it is made dense and sinks before moving away from the sites of the
45212 desalination plants towards the Strait of Hormuz.

46
47
48213 As the imposed salinity forcing increases, we observe stronger outflow of saltier, warmer and
49
50214 denser waters from the Gulf into the Sea of Oman through the Strait of Hormuz, which is
51
52215 balanced by stronger inflow of relatively fresher, cooler waters (Figure 3(e-g) and 4(e-g)).
53216 Vertical cross-sections through the Strait of Hormuz reveal that anomalously salty water exits
54
55217 the Gulf at depth on the southern side of the Strait, with fresher water being drawn in to the
56
57218 north near the surface. The main changes are in the salinity and exchange. The anomalies are
58
59219 most pronounced toward the bottom because the products of the desal plants are salty and
60
61220 dense.

3.2 Temperature and Salinity

The impact of desalination plants on the surface and bottom S and T grows with the capacity of the desalination plants. At present day levels of desalination (x1) there is limited impacts on the surface and bottom S and T (not shown). As desalination rates increase to 10-fold (x10), the SST changes are still less than 0.2°C in the Gulf, while there is a tendency of cooling in the eastern part of the Gulf (Figure 3(a)). This is likely due to cooler water being drawn into the Gulf from the Sea of Oman through the Strait of Hormuz. In addition, there is a noticeable increase in the bottom temperature by greater than 1°C near the sites of desalination plants, which is advected towards deeper regions (Figure 3(c)).

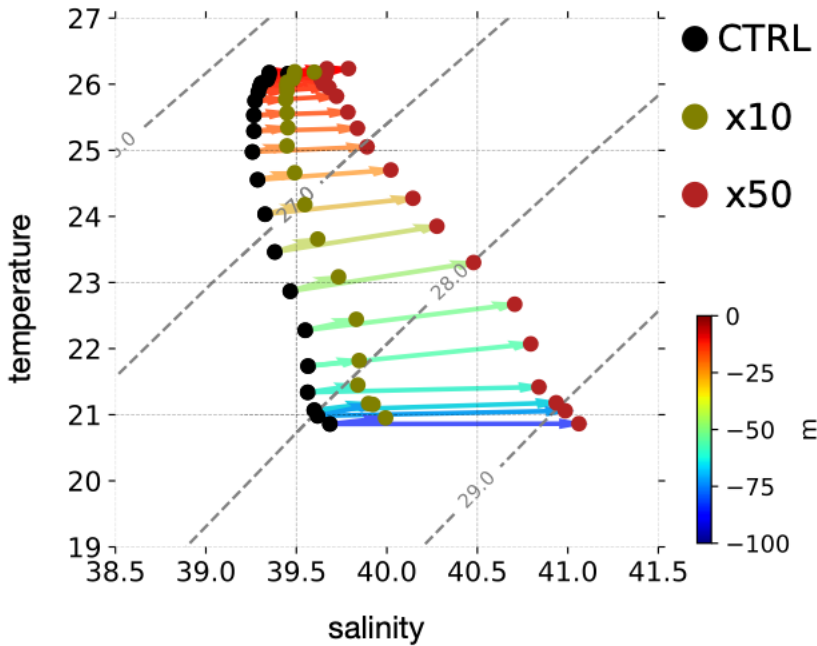
In the extreme 50-fold case (x50), we see a distinct line – what may be called a ‘flushing line’ – along which warm (and salty) waters leave the Gulf (Figure 4(c)). The temperature anomalies at the surface are comparable with those in x10, showing generally less than 0.2°C in the Gulf (Figure 4(a)). However, the bottom temperature anomalies exceed 2°C near the sites of desalination plants and gradually decreases along the flushing line as the water mass moves away from there (Figure 4(c)). This suggests that there is an active sink of warm water at the desalination plants which flows out of the Gulf mainly along the slope of bathymetry. There is also significant increase of temperature near the southern part of the Strait of Hormuz, suggesting that the temperature of the outflow is increased by up to 1°C (Figure 5(j)).

The salinity anomalies reveal clear patterns caused by brine discharge. In x10, the surface salinity anomalies increase reaching their maximum along the southern shoreline: 0.5 – 2 psu, and even greater than 2 psu in the east of Qatar (Figure 3(b)). The bottom salinity increases even more, showing broader areas with the salinity anomalies greater than 0.5 psu near the southern shoreline (Figure 3(d)). The positive salinity anomalies extend to the southern part of the Strait of Hormuz, showing the exit of salty water mass into the Sea of Oman.

The positive salinity anomalies are significant in the 50-fold scenario, particularly near the bottom of the Gulf (Figures 4(b,d)). At the surface, the inflow into the Gulf experiences the increasing salinity anomalies which can be greater than 2 psu near the desalination plants (Figure 4(b)). The bottom salinity anomalies significantly exceed 2 psu near the desalination plants. This salty water flows eastward, eventually leaving the Gulf through the southern part of the Strait of Hormuz (Figure 4(d)). Again, the region on the west, close to Qatar exhibits a

1
2
3 252 salinity increase which is much larger than 2 psu because of poor flushing as evidenced by the
4
5 253 anomalous current which flows toward the coast.
6

7 254 The size of salinity and temperature anomalies generally grows with depth, resulting in
8
9 255 stronger stratification (Figure 5). The increase of the vertical stability is particularly significant
10
11 256 in x50 where the bottom density increases approximately 1 kg/m^3 , while the surface density
12
13 257 rises by less than 0.5 kg/m^3 . This is primarily driven by the increase of salinity. The median
14
15 258 salinity near 100 m is nearly 1.5 psu greater in x50 than in CTRL, which is more than three
16
17 259 times the size of anomaly at the surface. This is somewhat expected as the desalination plants
18
19 260 transform the water mass towards higher density classes, indicating that their impacts
20
21 261 accumulate near the bottom of the Gulf. These changes also suggest that the increasing
22 262 capacity of the desalination plants in the Gulf exerts higher pressure on the marine environment
23
24 263 near the bottom.
25
26
27
28
29



30
31
32
33
34
35
36
37
38
39
40
41
42
43
44
45
46
47
48
49 264
50
51
52 265 **Figure 5. The median values of temperature and salinity in CTRL (black dots), x10 (olive**
53 266 **dots) and x50 (red dots) at each vertical level. The arrows and their colors represent changes**
54 267 **of water properties as a function of desalination forcing and depth, respectively.**
55

56
57 268 **3.3 Changes in overturning circulation**
58

59 269 Upon introduction of local salinity forcing from desalination plants, comparison of the
60
61 270 anomaly from x50 in Figure 8(a,b) with the CTRL in Figure 2(c,d), shows that the patterns
62
63
64
65

1
2
3 271 and sense of the overturning circulation -- both in the meridional and zonal directions --
4
5 272 remains the same but becomes stronger. Measures of the strength of these overturning
6
7 273 circulations as a function of desal strength is plotted in Figure 6(c,d). Most of the changes
8
9 274 occur in the northern and western regions of the Gulf. We observe a broad increase in the
10
11 275 strength of these overturning cells, and the change does not ‘level out’ even for x50, at which
12
13 276 point overturning strength approaches 50% of the mean. This supports the ‘flushing’
14
15 277 hypothesis of Ibrahim and Eltahir (2019) that the Gulf can efficiently exchange waters with
16
17 278 the Sea of Oman buffering interior change.

18
19 279 Interestingly, the overturning circulation in the Sea of Oman has also intensified in x50 (Figure
20
21 280 6(a)). This change is greater than in the Gulf, showing approximately a 100% increase
22
23 281 compared to CTRL (Figure 6(f)). The anomalous streamfunction extends deeper than 200 m
24
25 282 in the Sea of Oman, indicating that the outflow from the Gulf can sink deeper in x50 than in
26
27 283 CTRL due to the increased salinity of the outflow from the Gulf. At the surface, the westward
28
29 284 flow towards the Gulf has been intensified with the increased desalination capacity. Hence,
30
31 285 the enhanced overturning circulation in the Sea of Oman supports a more efficient exchange
32
33 286 of the water in the Gulf.

34 287 **3.4 Changes in the water-mass transformation rates**

35
36
37 288 Quantification of the water mass transformation rate – that is the rate at which the density of
38
39 289 water is changed from one value to another – is discussed at length in Al Shehhi, 2021 for our
40
41 290 CTRL scenario in which any local (desalination plant) salinity forcing was absent. In the
42
43 291 annual-average, the Gulf has a positive water-mass transformation rate both by surface heat
44
45 292 and freshwater fluxes (Figure 7(a,b)), meaning that water is converted from lighter density
46
47 293 classes to heavier ones. The largest contribution for the positive transformation rate is the latent
48
49 294 heat flux followed by longwave radiation (Figure 7(c)). In the Gulf, evaporation exceeds
50
51 295 precipitation (the latter is negligible) thus increasing the density of surface waters in the Gulf.
52
53 296 The shortwave radiation, however, lowers the density which largely compensates for the
54
55 297 density increase by both longwave and latent heat flux combined, leading to both positive and
56
57 298 negative values in the Gulf. On the other hand, the density increase by the freshwater flux is
58
59 299 positive in most parts of the Gulf, resulting in greater contribution to the total water mass
60
61 300 transformation rate.

62 301

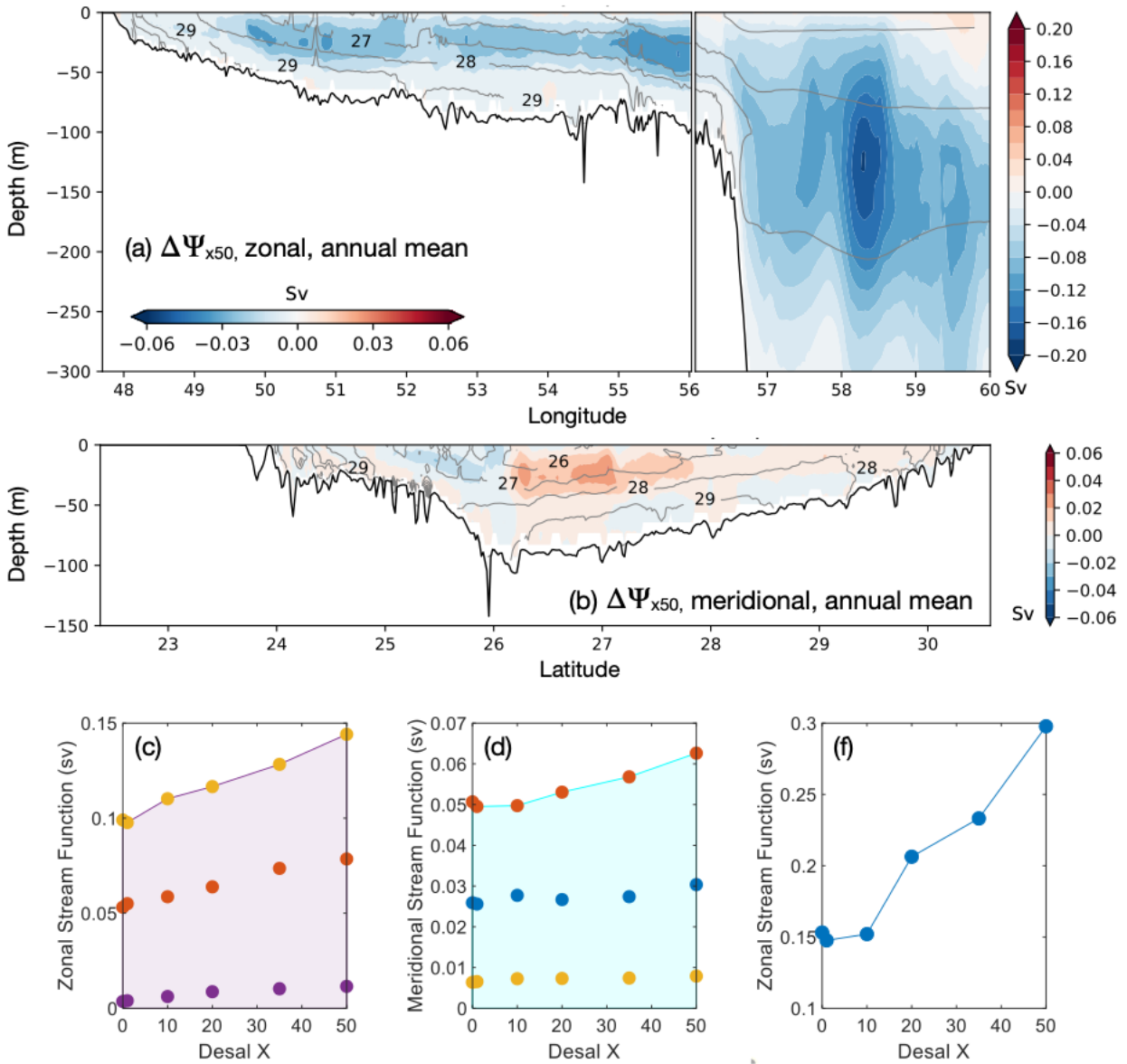


Figure 6. The anomaly of the residual streamfunction in (a) zonal and (b) meridional directions, respectively, for x50 compared to CTRL. There is anomalous anticlockwise circulation around the negative anomaly of the streamfunction. (c) Zonal streamfunction (Sv) at different locations in the Arabian Gulf for CTRL, x1, x10, x20, x35 and x50. The yellow color represents the eastern part of the Gulf, the blue color represents the center and the purple color represents the western part, (d) Meridional streamfunction (Sv) at different locations in the Arabian Gulf for CTRL, x1, x10, x20, x35 and x50. The orange, blue and

1
2
3
4
5
6
7
8
9
10
11
12
13
14
15
16
17
18
19
20
21
22
23
24
25
26
27
28
29
30
31
32
33
34
35
36
37
38
39
40
41
42
43
44
45
46
47
48
49
50
51
52
53
54
55
56
57
58
59
60
61
62
63
64
65

yellow dots represent the southern, central and northern part of the Gulf, and (c) the zonal stream function (Sv) at the strait of Hormuz for CTRL, x1, x10, x20, x35 and x50.

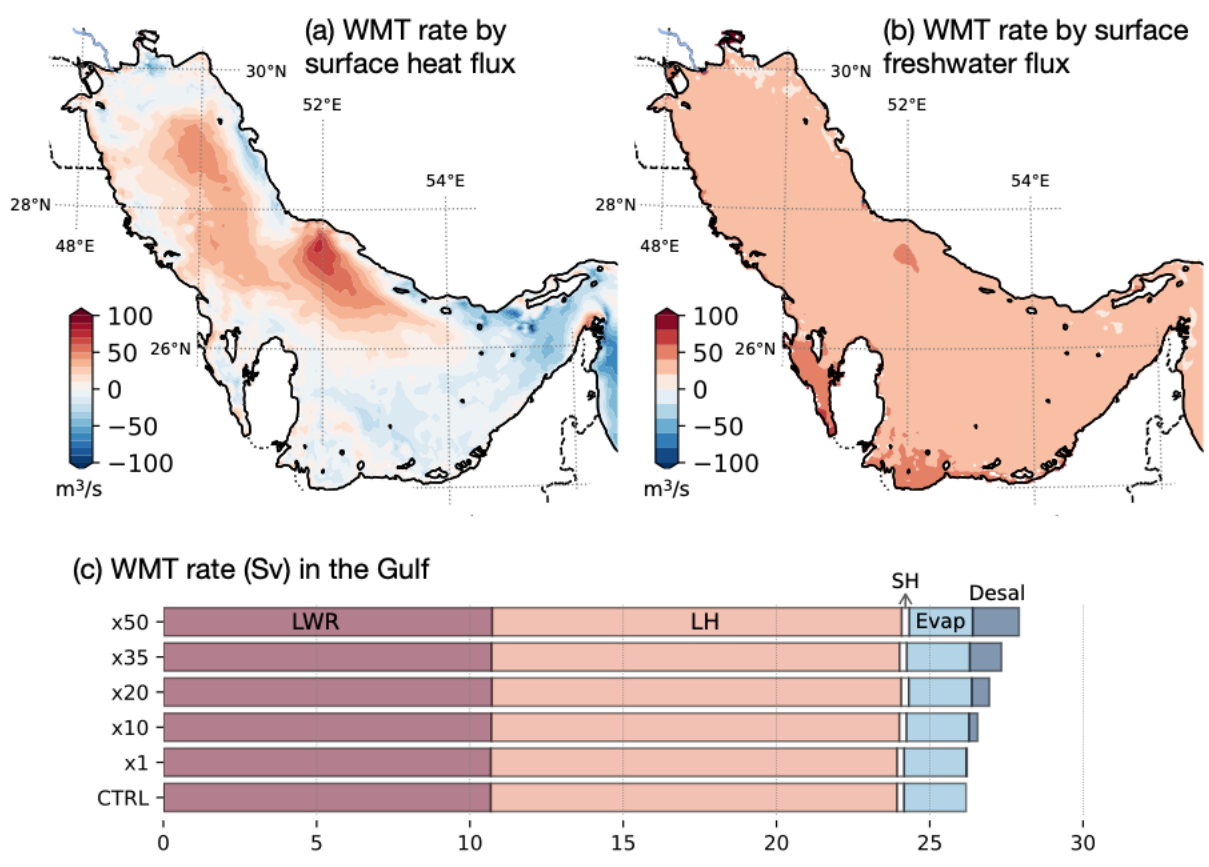


Figure 7. Water mass transformation rate (m³/s) by the surface (a) heat flux and (b) freshwater flux in CTRL. (c) The total water mass transformation rate by longwave radiation (LWR), latent heat flux (LH), sensible heat flux (SH), evaporation (Evap), and desalination plants (Desal) in the Gulf.

The introduction of forcing does not change the broad pattern of water mass transformation. However, there are significant increases, by as much as 100 m³/s, close to the desalination plants (not shown). When integrated over the whole Gulf, desalination plants rarely alter the water mass transformation rate contributed by heat and freshwater fluxes. In x50, however, the contribution from a few desalination plants to the transformation rate becomes comparable to that of evaporation over the whole Gulf region (Figure 7(c)). The increasing transformation rate due to desalination is consistent with the pattern of anomalous surface currents: the positive anomalies in the transformation rates (or increased diapycnal volume flux towards higher density) align well with the anomalous surface current observed in x10 and x50 (see Figure 3(a,b) and 4(a,b)).

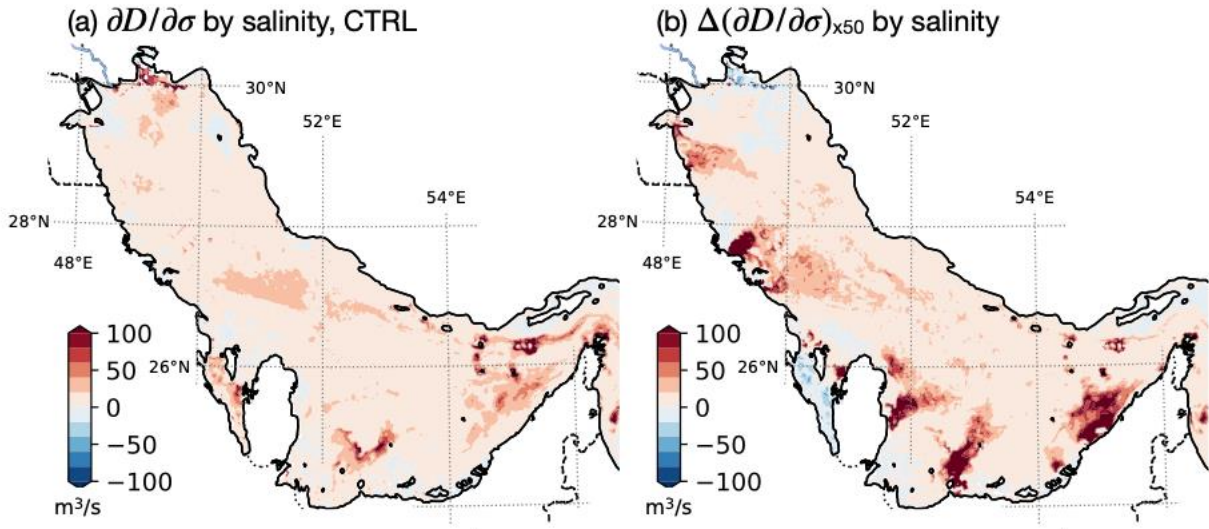


Figure 8. (a) Transformation rate by the diffusive salt flux below the surface ($\partial D/\partial\sigma$). (b) The difference of $\partial D/\partial\sigma$ between x50 and CTRL.

The positive water mass transformation rate due to diffusive salt flux below the surface layer can increase the density of the surface layer, though it is generally small compared to the surface buoyancy flux (Figures 7(a,b) and 8(a)). However, in certain regions, larger localized transformation can occur where the KPP boundary layer scheme can generate significantly enhanced localized diffusivities and mixing of salt. With the introduction of desalination plant forcings, the localized mixing by salt increases the density at the surface, particularly near the desalination plants in x50 (Figure 8(b)). The anomalous transformation rate by the salt mixing exceeds $100 \text{ m}^3/\text{s}$, and the contribution from diapycnal salt mixing to the surface layer density increase is greater than that from surface buoyancy fluxes. The positive anomalous transformation rate is also seen along the flushing line before the salty water from the desalination plants sinks away to depth. Given that the Gulf has a relatively uniform vertical profile in winter, this warm and salty water has the potential to increase the surface density.

4 Discussion and conclusions

The overall impact of salinity forcing from desalination plants across the Arabian Gulf has been assessed through application of a 3D regional model based on the MITgcm. Four major rivers and several desalination plants in the Gulf region were considered in the six scenarios: no desalination plant forcing, existing scenario (1-fold), 10-fold, 20-fold, 35-fold and 50-fold increases. Our desalination plant forcing was found to increase the salinity by approximately

1
2
3 348 0.2 g/kg and over 3 g/kg along the Gulf coast for the entire Gulf in the most extreme scenario.
4
5 349 Particularly significant increases in salinity were observed in shallow regions near the coasts
6
7 350 of Qatar and Bahrain where the circulation is weak and exchange with the interior Gulf limited.
8
9 351 In addition, an increase in the depth-averaged temperature up to 0.2-1.0 °C near the discharge
10
11 352 area of the desalination plants was noted, in Kuwait, Saudi and in the nearshore area of the
12
13 353 United Arab Emirates. A significant increase in the mean surface salinity and bottom
14
15 354 temperature is observed during the summer months when strong stratification suppresses
16
17 355 vertical mixing. In winter, brine is more uniformly mixed through the water column. Most of
18
19 356 the impact of brine discharge on the salinity and temperature, however, occurs on regional
20
21 357 scales within 2 to 3 kilometers from where the discharge occurs. the offshore areas are less
22
23 358 affected and response rather muted even in the most extreme desal rates considered.

24
25 359 We also find impacts on the horizontal and vertical overturning circulations. As desalination
26
27 360 rates are increased, fresher water is drawn into the Gulf more through the northern, surface
28
29 361 regions of the Strait. This leads to an anticlockwise anomalous cell which returns waters mid-
30
31 362 basin just north of the coastal shelf. Meanwhile salty waters are drawn over the shelf from the
32
33 363 desal plants operating on the southern coast. These sink to depth and exit the Gulf in a deep
34
35 364 salty anomaly to the south of the Strait. The associated overturning circulations retain the
36
37 365 same broad patterns but increase in strength reaching 50% of the mean in the 50-fold scenario.
38
39 366 This attests to the efficiency of the exchange which mutes the large-scale response of
40
41 367 temperature and salinity.

42 368 **5 Conflict of Interest**

43
44
45 369 *The authors declare that the research was conducted in the absence of any commercial or*
46
47 370 *financial relationships that could be construed as a potential conflict of interest.*

48 49 371 **6 Acknowledgments**

50
51
52 372 The authors acknowledge Khalifa University for its generous financial support and HPC Khal-
53
54 373 University for the Model run. JM and JS acknowledge support from MIT and the NASA
55
56 374 Physical Oceanography program. H. Song is grateful for the support by National Research
57
58 375 Foundation of Korea (NRF) Grant (NRF-2022R1A2C1009792 and 2018R1A5A1024958).

1
2
3377 **7 Reference**
4

- 5
6378 Abd El Wahab, M., and Hamoda, A. Z. (2012). Effect of desalination plants on the marine
7
8379 environment along the Red sea, Egypt.(case study). *Thalassas* 28, 27–36.
9
- 10380 Clark, G. F., Knott, N. A., Miller, B. M., Kelaher, B. P., Coleman, M. A., Ushiyama, S., et al.
11
12381 (2018). First large-scale ecological impact study of desalination outfall reveals trade-offs in
13
14382 effects of hypersalinity and hydrodynamics. *Water Res.* 145, 757–768.
15
- 16383 Danoun, R. (2007). Desalination Plants: Potential impacts of brine discharge on marine life.
17
18
- 19384 Egbert, G. D., Bennett, A. F., and Foreman, M. G. G. (1994). TOPEX/POSEIDON tides
20
21385 estimated using a global inverse model. *J. Geophys. Res. Ocean.* 99, 24821–24852.
22
- 23
24386 Einav, R., Harussi, K., and Perry, D. (2003). The footprint of the desalination processes on the
25
26387 environment. *Desalination* 152, 141–154.
27
- 28388 Hosseini, H., Saadaoui, I., Moheimani, N., Al Saidi, M., Al Jamali, F., Al Jabri, H., et al. (2021).
29
30389 Marine health of the Arabian Gulf: Drivers of pollution and assessment approaches
31
32390 focusing on desalination activities. *Mar. Pollut. Bull.* 164, 112085.
33
- 34
35391 Le Quesne, W. J. F., Fernand, L., Ali, T. S., Andres, O., Antonpoulou, M., Burt, J. A., et al.
36
37392 (2021). Is the development of desalination compatible with sustainable development of the
38
39393 Arabian Gulf? *Mar. Pollut. Bull.* 173, 112940.
40
- 41394 Marshall, J., Adcroft, A., Hill, C., Perelman, L., and Heisey, C. (1997). A finite-volume,
42
43395 incompressible Navier Stokes model for studies of the ocean on parallel computers. *J.*
44
45396 *Geophys. Res. Ocean.* 102, 5753–5766.
46
- 47397 Missimer, T. M., and Maliva, R. G. (2018). Environmental issues in seawater reverse osmosis
48
49398 desalination: Intakes and outfalls. *Desalination* 434, 198–215.
50
- 51
52399 Panagopoulos, A., Haralambous, K.-J., and Loizidou, M. (2019). Desalination brine disposal
53
54400 methods and treatment technologies-A review. *Sci. Total Environ.* 693, 133545.
55
- 56401 Paparella, F., D’Agostino, D., and Burt, J. (2022). Long–Term, Basin–Scale Salinity Impacts
57
58402 from Desalination in the Arabian/Persian Gulf.
59
- 60
61403 Purnama, A. (2021). “Assessing the Environmental Impacts of Seawater Desalination on the
62
63
64
65

1
2
3
4
5
6
7
8
9
10
11
12
13
14
15
16
17
18
19
20
21
22
23
24
25
26
27
28
29
30
31
32
33
34
35
36
37
38
39
40
41
42
43
44
45
46
47
48
49
50
51
52
53
54
55
56
57
58
59
60
61
62
63
64
65

Hypersalinity of Arabian/Persian Gulf,” in *The Arabian Seas: Biodiversity, Environmental Challenges and Conservation Measures* (Springer), 1229–1245.

Roberts, D. A., Johnston, E. L., and Knott, N. A. (2010). Impacts of desalination plant discharges on the marine environment: A critical review of published studies. *Water Res.* 44, 5117–5128.

Rocha, C. B., Chereskin, T. K., Gille, S. T., and Menemenlis, D. (2016). Mesoscale to submesoscale wavenumber spectra in Drake Passage. *J. Phys. Oceanogr.* 46, 601–620.

Ruso, Y. D. P., De la Ossa Carretero, J. A., Casalduero, F. G., and Lizaso, J. L. S. (2007). Spatial and temporal changes in infaunal communities inhabiting soft-bottoms affected by brine discharge. *Mar. Environ. Res.* 64, 492–503.

Saif, O. (2012). The Future Outlook of Desalination in the Gulf: Challenges & opportunities faced by Qatar & the UAE.

Sharifinia, M., Afshari Bahmanbeigloo, Z., Smith Jr, W. O., Yap, C. K., and Keshavarzifard, M. (2019). Prevention is better than cure: Persian Gulf biodiversity vulnerability to the impacts of desalination plants. *Glob. Chang. Biol.* 25, 4022–4033.

Smith, W. H. F., and Sandwell, D. T. (1997). Global sea floor topography from satellite altimetry and ship depth soundings. *Science* (80-.). 277, 1956–1962.

Sola, I., Fernández-Torquemada, Y., Forcada, A., Valle, C., del Pilar-Ruso, Y., González-Correa, J. M., et al. (2020). Sustainable desalination: Long-term monitoring of brine discharge in the marine environment. *Mar. Pollut. Bull.* 161, 111813.

1 Data Availability Statement

The full LLC4320 model setup with compile-time and run-time parameters can be found at http://wwwcvs.mitgcm.org/viewvc/MITgcm/MITgcm_contrib/llc_hires/llc_4320/.

Declaration of interests

The authors declare that they have no known competing financial interests or personal relationships that could have appeared to influence the work reported in this paper.

The authors declare the following financial interests/personal relationships which may be considered as potential competing interests: